Journal of Applied Physics ARTICLE pubs.aip.org/aip/jap

Point defects in proton-irradiated highly Ga- and B-doped Ge

Cite as: J. Appl. Phys. **139**, 015703 (2026); doi: 10.1063/5.0305060
Submitted: 3 October 2025 · Accepted: 10 December 2025 ·
Published Online: 2 January 2026

Pejk Amoroso,[1,a)] Jonatan Slotte,[1,2] Aravind Subramanian,[3] Waldemar Särs,[1] Kenichiro Mizohata,[1] R. Radhakrishnan Sumathi,[3] and Filip Tuomisto[1]

AFFILIATIONS

[1]Department of Physics, University of Helsinki, P.O. Box 43, FI-00014 Helsinki, Finland
[2]Department of Applied Physics, Aalto University, P.O. Box 15100, FI-00076 Aalto, Finland
[3]Leibniz-Institut für Kristallzüchtung (IKZ), Max-Born-Str. 2, 12489 Berlin, Germany

[a)]**Author to whom correspondence should be addressed:** pejk.amoroso@helsinki.fi

ABSTRACT

In this study, point defects in highly Ga- and B-doped Ge bulk crystalline samples were investigated using Positron Annihilation Lifetime Spectroscopy. The samples were irradiated with 6 MeV protons at room temperature up to a fluence of 3×10^{14} cm^{-2} in order to produce vacancy-type defects along the ion track. Initially after irradiation, vacancy-dopant complexes are observed in all samples. However, measurements performed a year after irradiation suggest evolution of the defects, indicating a low binding energy between the vacancy and the dopants. An increase in the size of the vacancy-type defects is observed with increasing dopant concentration in the 5×10^{17}-, 1×10^{18}-, and 1×10^{19} cm^{-3}-doped samples. Interestingly, the defect lifetime component for the 1×10^{20} cm^{-3} Ga-doped sample is significantly lower than in the less-doped samples, which is concluded to be a result of a high concentration of negative ions complicating decomposition of the spectra. Temperature-dependent measurements show evidence in support of this conclusion, while also observing an abnormal positron annihilation state characterized by a lifetime below that in defect-free bulk.

I. INTRODUCTION

In the first decade of semiconductor electronics, germanium (Ge) was being considered as a potential candidate for mainstream applications. However, silicon (Si) emerged as a superior material due to many advantages, including significantly lower cost and higher thermal stability. Interest in Ge as a research topic dropped, while the rise of Si as the dominating semiconductor material for electronics meant that its properties have been studied extensively. However, in the effort to develop faster electronic components, Ge has in recent years emerged as a promising material mainly due to having a higher carrier mobility and lower dopant activation temperatures than Si.[1] This emergence has revitalized Ge as a subject of research, as crucial properties relating to point defects are still unknown.

Highly doped Ge is a promising material for mid-infrared detectors, bio-sensors, and CMOS devices.[2,3] Typically, high doping levels are achieved using ion implantation or epitaxial growth. Optimizing the process of producing such materials using bulk growth methods, such as the Czochralski technique, would facilitate the fabrication at large scales to meet an increasing demand. By introducing dopants in the melt to grow doped bulk crystals, it is possible to avoid defect formation originating from post-growth doping techniques, such as ion implantation, which usually requires an additional step involving thermal annealing to reduce the defect density. However, point defects inevitably form during Ge crystal pulling, and doping further affects defect formation.[4]

Point defects can limit device functionality, as they can act as carrier traps, deactivate dopant atoms, and impact dopant diffusion. While point defects in Si are fairly well understood, the same cannot be said about Ge. Even though Ge and Si share many material properties, such as being elemental semiconductors with indirect bandgaps, and both having a diamond lattice structure, it has become clear that point defect-dopant interactions differ significantly. While self-diffusion in Si is mediated by both vacancies and

interstitials in almost equal magnitudes,[5] it is vacancy-mediated in Ge, which has a lower vacancy formation energy than Si.[6,7] DFT calculations indicate that the formation enthalpy of the vacancy (V) is lower than for the interstitial (I) in Ge.[8] As a consequence, the self-diffusion[9] and diffusion of most dopants, including Ga, are vacancy-mediated in Ge under thermal equilibrium.[10,11] An exception to this is B, which is interstitial-mediated.[12] On the other hand, DFT calculations have indicated that Ga- and B-doping during growth could result in interstitial-rich Ge crystals.[13] However, under concurrent irradiation conditions, diffusion of dopants is interstitial-mediated, as a supersaturation of interstitials is established due to the Ge surface being an insufficient sink for Ge interstitials, while the vacancy concentration is kept at thermal equilibrium.[14,15] The formation of dopant-defect complexes seems to induce dopant deactivation to a greater extent in Ge[16,17] than in Si.[18]

While diffusion mechanisms in Ge are well understood, characterization of dopant-vacancy complexes in p-type Ge remains to be studied. The vacancy in Ge can exist in different charge states,[19,20] which complicates the analysis, as it is known that vacancy-impurity interactions and the relaxation of the lattice surrounding the vacancy depend on the charge state. While research suggests that Ga atoms are attracted to vacancies in Ge,[11,21] DFT calculations indicate that B is electrostatically repelled by the vacancy in Ge.[22,23]

In this study, we use proton irradiation to produce vacancy-type defects in bulk-grown highly p-type Ge. We employ positron annihilation lifetime spectroscopy (PALS) to study the role of dopant and dopant concentration on the formation of vacancy-type defects, as well as discuss the presence of shallow positron traps. PALS is a useful tool for characterizing neutral and negatively charged open volume defects in the range of 10^{15}--$10^{19}\,\mathrm{cm}^{-3}$, as well as negative ions (shallow positron traps). However, PALS is not suitable for studying positively charged defects, which is one of the reasons why p-type Ge has not been studied using this method. Interestingly, open volume defects are observed post-irradiation in both Ga- and B-doped p-type Ge in this work. Hence, we show that the vacancy-type defects are neutral or negatively charged. The observation of open volume defects in the B-doped sample suggests V-B complex formation. This is possibly due to the irradiation, causing the Fermi level to rise, thus changing the charge state of the vacancy. In addition, hints of divacancy-size open volumes are observed in the lifetime results, thereby suggesting the presence of divacancy complexes, which have been found to be stable at RT by several studies.[24–27] In this study, measurements done a year post-irradiation show a decrease in positron lifetime after annealing the samples at 400 K, which suggest either a lower concentration of vacancy-type defects or a decrease in the volume of these defects.

II. EXPERIMENTAL DETAILS

The samples investigated in this study included heavily B-doped Ge and Ga-doped Ge. B-doped samples, measuring $7 \times 7 \times 0.6\,\mathrm{mm}^3$, and Ga-doped samples, measuring $10 \times 10 \times 1\,\mathrm{mm}^3$, were obtained from the bulk single crystals along the axial direction (parallel to the growth axis). The bulk crystals were grown using the Czochralski technique along the ⟨100⟩ direction. For the crystal growth, high purity Ge feed material (>7N) along with metallic Ga (>5N) and B (>5N) granules was loaded into a quartz crucible to produce Ge:Ga and Ge:B bulk single crystals, respectively. Further details regarding the growth experiment can be found in Refs. 28 and 29.

The axial distribution of dopant concentrations along the length of the crystals was determined using the secondary ion mass spectroscopy and the μ-x-ray fluorescence techniques.[28,29] Furthermore, the electrically active charge carrier concentrations of the investigated samples were measured using the Hall measurement technique. The selected B-doped samples exhibited an active charge carrier concentration of $5 \times 10^{17}\,\mathrm{cm}^{-3}$ ($\pm 0.1\%$), while the Ga-doped samples displayed active charge carrier concentrations of $1 \times 10^{18}\,\mathrm{cm}^{-3}$ ($\pm 0.05\%$), $1 \times 10^{19}\,\mathrm{cm}^{-3}$ ($\pm 0.05\%$), and $1 \times 10^{20}\,\mathrm{cm}^{-3}$ ($\pm 0.1\%$), respectively. The chemically determined dopant concentrations and the electrically active carrier concentrations closely agree, suggesting near complete dopant activation in the crystals. For clarity, the samples will hereafter be referred to according to their respective electrically active charge carrier concentrations.

Impurity concentrations in the Ga-doped samples were investigated using time-of-flight elastic recoil detection analysis with a 40 MeV ^{127}I beam. No impurity concentrations exceeding the detection limit of ∼0.1 at. % were identified. Furthermore, Particle-Induced X-ray Emission (PIXE) analysis determined the total dopant concentration in the $1 \times 10^{20}\,\mathrm{cm}^{-3}$ Ga-doped sample to be $1.06 \times 10^{20}\,\mathrm{cm}^{-3}$, which is in good agreement with the Hall measurements.

Vacancy-type defects were characterized using Positron Annihilation Lifetime Spectroscopy (PALS) in two different fast–fast coincidence setups. Room-temperature (RT) measurements were performed in a PALS setup with BaF_2 scintillators coupled to photomultiplier tubes (PMTs), with a resolution of 280 ps. Temperature-dependent measurements were performed in a PALS setup with plastic scintillators coupled to PMTs, with a resolution of 260 ps. The samples were mounted in a conventional sandwich geometry, with a 1.5 MBq e^+-source of ^{22}NaCl wrapped in a 1.5 μm Al foil. For the temperature-dependent measurements, the sandwich was mounted on a copper holder in thermal contact with a closed-cycle helium cryostat. Prior to the analysis, lifetime components stemming from annihilation events in the source, in the Al foil and as positronium, were subtracted from the lifetime spectra.

The samples were irradiated uniformly across the entire sample surface with 6 MeV protons at RT. Since the goal of this work was to characterize and quantify vacancy-type defects, the energy and fluence were chosen such that (i) mainly primary defects are created, (ii) end-of-range defects occur beyond the depth of positron implantation, and (iii) positron saturation trapping, where all annihilation events originate from trapped positrons, is avoided.[30] Based on SRIM simulations,[31] the projected range of the 6 MeV protons is approximately 185 μm in Ge. The average positron implantation depth in Ge is 50 μm. Hence, a negligible fraction of positrons probe the end-of-range defects. The concentration of vacancies produced by irradiation was calculated according to the conventional procedure.[32]

The samples were irradiated in two steps. First, the samples were irradiated with a fluence of $1 \times 10^{14}\,\mathrm{cm}^{-2}$, after which they were measured using an *ex situ* PALS setup at room temperature. The samples were then irradiated a second time with a fluence of

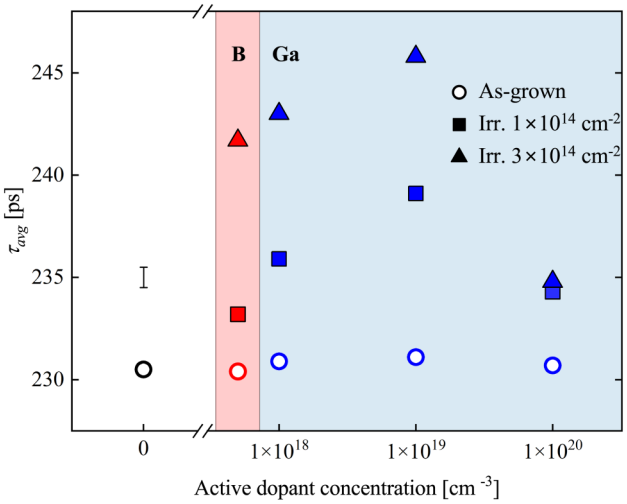

FIG. 1. Average positron lifetime at room temperature as a function of active dopant concentration. The statistical error in average lifetime is of the order of 1 ps.

2×10^{14} cm^{-2}, amounting in a total fluence of 3×10^{14} cm^{-2}, and again measured with *ex situ* PALS. The proton irradiation caused some activation of the sample. To avoid unwanted influence from the decaying As isotopes, we waited at least 96 h post-irradiation before starting PALS measurements.

The temperature-dependent measurements were performed approximately 12 months post-irradiation. The samples were cooled down to 50 K, after which they were measured with increasing temperature up to 400 K, and finally with decreasing temperature down to 50 K. The B-doped sample was measured twice as a function of temperature in order to investigate a potential lattice recovery observed during the first measurement series.

III. RESULTS

Figure 1 shows the average positron lifetime at room temperature (~295 K) before and after irradiation of the *p*-type samples, as well as for an as-grown positron-trap free Ge reference sample. The as-grown *p*-type samples show no signs of detectable open volume defects. The proton irradiation creates neutrally or negatively charged vacancy-type defects, as is seen by the increase in average positron lifetime. The average positron lifetime increases with increasing doping concentration for the three lower-doped samples, but is surprisingly low for the highest-doped sample.

Figure 2 shows the decomposed lifetime components, with τ_1 and τ_2 representing the reduced bulk lifetime and the defect lifetime component, respectively. The dashed line in the τ_2 plot is the defect lifetime component for the monovacancy in Ge, while the grayed area encloses values found for different charge states of the divacancy.[24,26] After the first irradiation fluence of 1×10^{14} cm^{-2}, the τ_2 component for the B-doped sample is approximately that of the isolated monovacancy and higher for the 1×10^{18} cm^{-3} and 1×10^{19} cm^{-3} Ga-doped samples. Two clear lifetime components

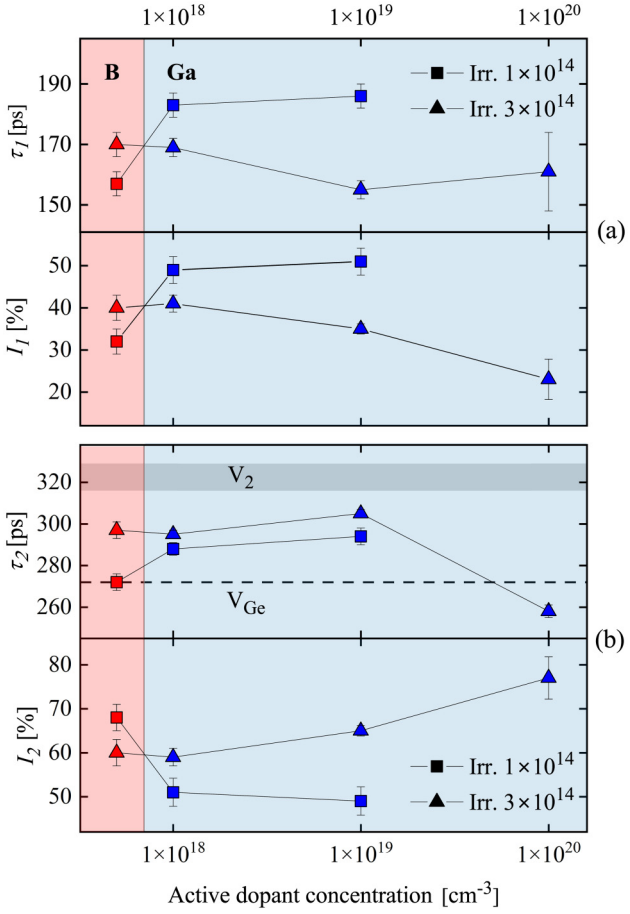

FIG. 2. The decomposed lifetime spectrum at room temperature. (a) The reduced bulk lifetime component τ_1, as well as the intensity I_1 of the component as a function of active dopant concentration. (b) The defect lifetime component τ_2, as well as the intensity I_2 of the component as a function of active dopant concentration. The dashed line and the grayed area mark the defect lifetime component of the monovacancy and divacancy in Ge, respectively. The result for the 1×10^{14}-irradiated and 1×10^{20} cm^{-3}-doped sample has been left out due to the large uncertainty.

could not be resolved from the lifetime spectrum of the highest-doped sample after the first irradiation dose. The second irradiation dose increased the vacancy concentration, allowing decomposition of the spectrum into two separate lifetime components. After the second irradiation dose, τ_2 is approximately 300 ps for the 5×10^{17}--1×10^{19} cm^{-3}-doped samples and 262 ps for the 1×10^{20} cm^{-3}-doped sample, which is lower than that of the monovacancy.

Figure 3 shows the average positron lifetime as a function of temperature. The dashed line represents the average positron lifetime of the reference Ge sample, which was found to remain unchanged across the whole temperature range. The average lifetime strongly increases with increasing temperature for all samples. In the B-doped and 1×10^{18} and 1×10^{19} cm^{-3} Ga-doped

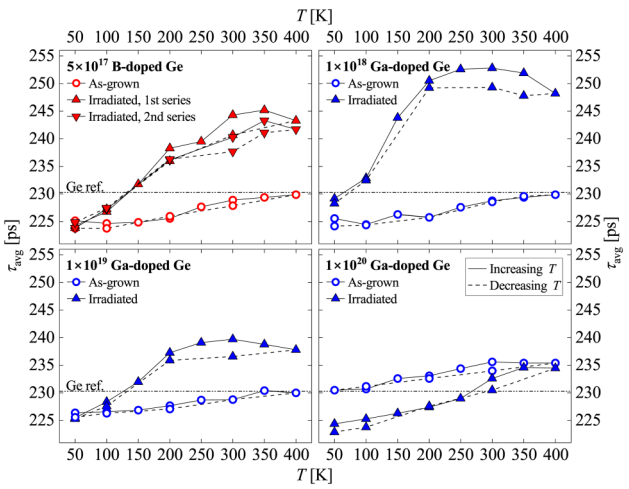

FIG. 3. Average positron lifetime of 3×10^{14} cm^{-2}-irradiated samples as a function of measurement temperature. The irradiated B-doped sample was measured twice. The temperature-dependent measurements were performed 1 year after the irradiation. The statistical error in average lifetime is of the order of 1 ps.

samples, the average lifetime ceases to increase at approximately RT and exhibits lower average lifetimes at $T > 200$ K when the temperature is decreased. Furthermore, a second temperature-dependent measurement of the B-doped sample yielded lower average lifetimes at $T > 200$ K compared to the first measurement series. The drop in average lifetime can be attributed to a reduction in open-volume defects due to the thermal history. This is discussed further in Sec. IV. Interestingly, in the 1×10^{20} cm^{-3} Ga-doped sample, the average lifetime increases over the whole temperature range and decreases along the same path when the temperature is decreased.

Figure 4 shows the decomposed lifetime spectra of the temperature-dependent measurements. Decomposition of the spectra of the 1×10^{19}- and 1×10^{20} cm^{-3} Ga-doped samples across the whole temperature range, as well as of the B-doped and 1×10^{18} cm^{-3} Ga-doped samples at $T < 200$ K, failed and have, thus, been excluded from the graph.

No clear evolution of the τ_2 component can be observed, nor a difference between the measurements with increasing and decreasing temperature. However, τ_2 is clearly higher compared to the RT measurements performed a year prior to the temperature-dependent measurements, which suggests that the V–A complexes produced by irradiation have migrated and formed stable open-volume defects with two or more vacancies. In addition, the τ_2 component of the B-doped sample is higher than that of the 1×10^{18} cm^{-3} Ga-doped sample.

IV. DISCUSSION

Since the isolated monovacancy in Ge is not stable at RT,[24] the vacancy-type defects observed in Figs. 1 and 2 are V–A complexes, or possibly divacancy complexes, which were found to be

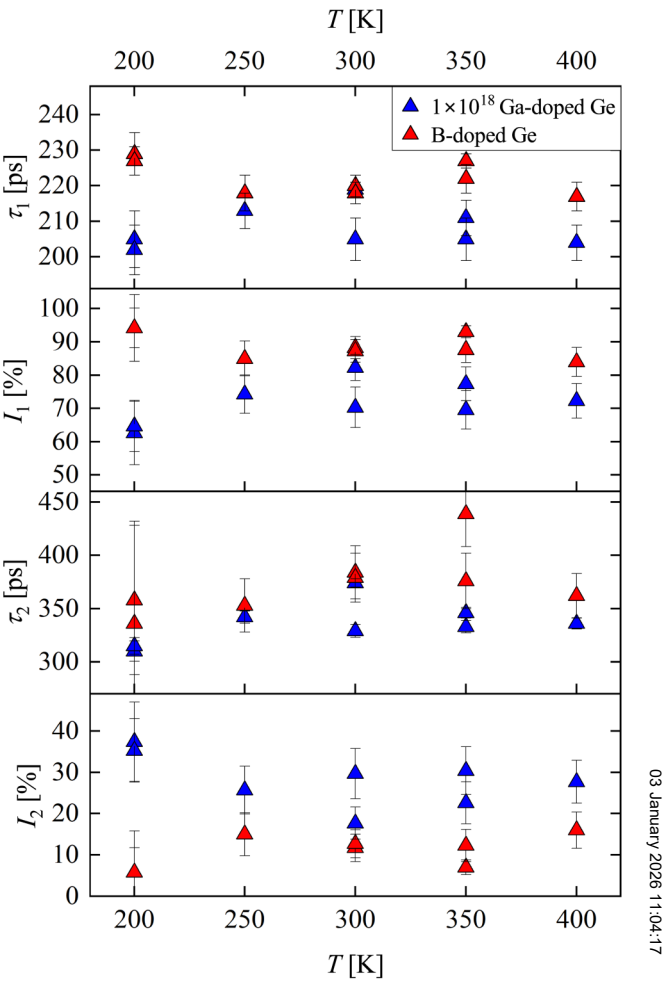

FIG. 4. The decomposed lifetime spectra of 3×10^{14} cm^{-2}-irradiated samples as a function of temperature. The temperature-dependent measurements were performed 1–year after the irradiation. Decomposition failed for the 1×10^{19}- and 1×10^{20} cm^{-3} Ga-doped samples, as well as for the B-doped and 1×10^{18} cm^{-3} Ga-doped samples at $T < 200$ K.

stable at RT by many studies.[24–27] However, other studies have failed to observe stable divacancy complexes at RT.[33] The formation of V–B complexes indicates that B is not repelled by the vacancy as previous calculations have suggested.[22] Since the concentration of vacancies produced ($>10^{16}$) is a magnitude lower than the B-concentration ($>10^{17}$), the irradiation could raise the Fermi level enough to change the charge state of the vacancy, allowing B–V complex formation. In the Ga-doped samples, the doping concentration is too high for the vacancies to noticeably move the Fermi level.

The increase in average positron lifetime with increasing dopant concentration is due to a higher probability of forming a complex before the vacancy recombines with an interstitial or migrates out of the sample. We suggest that the lower average

lifetime for the highest-doped sample is a result of a high concentration of shallow positron traps, resulting in a lower fraction of positrons being trapped in vacancy-type defects. The thermal energy of positrons at RT in most cases exceeds the binding energy of shallow positron traps, meaning that this type of trapping usually is only observed at low temperatures. Here, we argue that the high concentration of negative ions and high binding energy renders this effect visible even at room temperature.[34,35] The effect of shallow positron traps is supported by the strong temperature-dependent behavior observed in Fig. 3. Moreover, an important difference can be observed between the 5×10^{17}–1×10^{19} and the 1×10^{20} cm^{-3}-doped samples. While the lifetime in the 1×10^{20} cm^{-3}-doped sample increases over the whole temperature range, it stops increasing at approximately 300 K and starts decreasing in the 5×10^{17}–1×10^{19} cm^{-3}-doped samples. This supports the argument that the negative ion concentration is of importance for shallow positron trapping.

The failed decomposition over the whole temperature range for the 1×10^{19} and 1×10^{20} cm^{-3} Ga-doped samples and the failed decomposition at low temperatures for the B-doped and 1×10^{18} cm^{-3} Ga-doped samples further support the argument that at least three competing annihilation states exist: the temperature-dependent shallow positron trap, the defect-free bulk, and one or more types of open-volume traps.

Kuitunen *et al.* and Slotte *et al.* have shown that the divacancy in Ge is characterized by a defect lifetime component of 315–330 ps, depending on the charge state.[24,25] Considering this, the high defect lifetime component of approximately 300 ps seen in Fig. 2 could potentially in part be attributed to the presence of divacancy complexes, although the radiation fluence and energy were chosen such that mainly primary defects would be created. The presence of divacancy complexes could be explained by pre-existing positively charged vacancy-type defects in the as-grown samples, and thus invisible to PALS, which subsequently form divacancy complexes with monovacancies created during irradiation. Alternatively, the divacancy complexes could form as a result of defect evolution, where mobile monovacancies or *V*–*D* complexes produced by the irradiation would merge. Possible evidence of this is seen in Fig. 4 where a defect lifetime components of >300 ps are observed for the B-doped and 1×10^{18} cm^{-3} Ga-doped samples, that with reasonable certainty are larger than in the measurements a year prior.

Surprisingly, τ_2 for the highest-doped sample is clearly lower than for the isolated monovacancy, indicating less open volume. Three phenomena could explain this lower τ_2: (i) an inward relaxation of the dopant atoms, although this would be expected also in the 1×10^{18} and 1×10^{19} cm^{-3} Ga-doped samples; (ii) an absence of divacancy complexes, which, therefore, would be present in the 1×10^{18} and 1×10^{19} cm^{-3} Ga-doped samples with higher τ_2; and (iii) this is a result of shallow positron traps complicating decomposition of the spectra. Considering that decomposition into two lifetime components failed after the first irradiation dose, we suggest the latter explanation. As seen in Fig. 3, the positron lifetimes of both as-grown and irradiated *p*-type samples, except the as-grown 1×10^{20} cm^{-3} Ga-doped sample, drop below the positron trap-free Ge bulk lifetime at low temperatures. This indicates the existence of an annihilation state, where the electron density locally is higher than in the defect-free bulk, as the positron annihilation rate λ is proportional to the overlap of positron and electron densities,

$$\lambda = \frac{1}{\tau} = \pi r_0^2 c \int \gamma(\mathbf{r}) n_+(\mathbf{r}) n_-(\mathbf{r}) d\mathbf{r}, \quad (1)$$

where r_0 is the classical electron radius, c is the velocity of light, and $n_+(\mathbf{r})$ and $n_-(\mathbf{r})$ are the positron and electron densities. The enhancement factor $\gamma(\mathbf{r})$ takes into account the screening of positrons by electrons.

In order to eliminate the possibility that impurity-defect complexes commonly found in Czochralski-grown Ge, such as the *V*–*O* complex (also known as the *A*-center), may be responsible for the 5 ps decrease in positron lifetime at low temperatures, we also measured a high-purity Ge sample (HPGe) over the temperature interval 50–300 K. The average lifetime was found to be equal to that of the reference Ge sample over the whole temperature interval.

The temperature-dependent measurements were performed 1 year post-irradiation. When comparing the average positron lifetime in Figs. 1 and 3 at RT, and τ_2 in Figs. 2 and 4, it is clear that the samples have undergone structural change at RT. As seen in Fig. 3, heating up the B-doped and 1×10^{18} and 1×10^{19} cm^{-3} Ga-doped samples to 400 K did result in a decrease in average lifetime at RT, which could be explained by lattice recovery. This was confirmed by performing a second series of temperature-dependent measurements for the B-doped sample, in which a lower average lifetime is observed in the temperature range of 200–400 K. The increase in τ_2 suggests a low binding energy between the vacancy and the dopants, resulting in migration of the initial defects formed during irradiation until *V*-complexes with two or more vacancies are formed, which are characterized by a τ_2 of <300 ps.

Even though strong evidence in favor of negative ions trapping positrons is presented in this study, their presence remains somewhat mysterious. With the 1×10^{19} and 1×10^{20} cm^{-3} Ga-doped samples being degenerate, the large carrier concentration should screen any charged defects in the lattice. Still, the temperature-dependence observed cannot be explained by phenomena such as thermal expansion/contraction, as the undoped Ge sample exhibits no such temperature-dependent behavior. More in-depth studies are required to explain this effect.

V. SUMMARY

We have used proton irradiation to produce vacancy-type defects in highly *p*-type Ge and subsequently studied them using PALS. Although the exact characteristics of the defects remain elusive, we find an increase in the size and/or the quantity of RT-stable vacancy-type defects with increasing dopant concentration, in the 5×10^{17}, 1×10^{18}, and 1×10^{19} cm^{-3}-doped samples. Furthermore, the size of the vacancy-type defects is equal or larger in comparison to the isolated monovacancy in Ge.

Surprisingly, the open volume defects produced by the proton irradiation in the 1×10^{20} cm^{-3} Ga-doped sample appear smaller and/or fewer compared to the other samples, as well as compared to the isolated monovacancy in Ge. In temperature-dependent

positron lifetime measurements performed a year after the RT-measurements, we find evidence of shallow positron traps (typically negative ions), which are characterized by an increasing trapping rate with decreasing temperature. We suggest that the high concentration of shallow positron traps in the 1×10^{20} cm^{-3} Ga-doped sample complicates the decomposition of the spectra, thus rendering it difficult to determine whether the difference in the size of the open volume defects is real or a decomposition issue. In addition, we observe a change in both average positron lifetime and τ_2 compared to the initial RT-measurement, as well as a decrease in average positron lifetime after heating up the samples to 400 K, which suggests a low binding energy between the vacancy and the dopants. For the 1×10^{18} and 1×10^{19} cm^{-3} Ga-doped samples, for which two lifetime components could be resolved, we see evidence of an increase in the number of divacancy complexes. Finally, we observe a previously unobserved positron state resulting in a lifetime below the defect-free bulk at low temperatures.

ACKNOWLEDGMENTS

This material is based on work supported by the Air Force Office of Scientific Research under Award No. FA8655-22-1-7037. The authors acknowledge the financial support by the Vilho, Yrjö and Kalle Väisälä Foundation of the Finnish Academy of Science and Letters. The authors A.S. and R.R.S. acknowledge the German Research Foundation (DFG—Grant No. 509113935) for the financial support.

AUTHOR DECLARATIONS

Conflict of Interest

The authors have no conflicts to disclose.

Author Contributions

Pejk Amoroso: Conceptualization (supporting); Data curation (equal); Formal analysis (lead); Funding acquisition (supporting); Investigation (lead); Project administration (supporting); Visualization (lead); Writing – original draft (lead); Writing – review & editing (supporting). **Jonatan Slotte:** Conceptualization (lead); Formal analysis (supporting); Investigation (supporting); Project administration (lead); Resources (supporting); Supervision (lead); Visualization (supporting); Writing – original draft (supporting); Writing – review & editing (lead). **Aravind Subramanian:** Formal analysis (supporting); Funding acquisition (supporting); Investigation (supporting); Resources (supporting); Writing – original draft (supporting); Writing – review & editing (supporting). **Waldemar Särs:** Formal analysis (supporting); Investigation (supporting). **Kenichiro Mizohata:** Data curation (supporting); Formal analysis (supporting); Investigation (supporting); Writing – review & editing (supporting). **R. Radhakrishnan Sumathi:** Conceptualization (supporting); Funding acquisition (supporting); Project administration (supporting); Resources (supporting); Writing – review & editing (supporting). **Filip Tuomisto:** Conceptualization (supporting); Funding acquisition (lead); Resources (equal); Supervision (supporting); Writing – review & editing (supporting).

DATA AVAILABILITY

The data that support the findings of this study are available from the corresponding author upon reasonable request.

REFERENCES

[1]C. Claeys and E. Simoen, *Germanium-Based Technologies* (Elsevier, 2007).
[2]G. Pellegrini, L. Baldassare, V. Giliberti, J. Frigerio, K. Gallacher, D. J. Paul, G. Isella, M. Ortolani, and P. Biagioni, "Benchmarking the use of heavily doped ge for plasmonics and sensing in the mid-infrared," ACS Photonics **5**, 3601–3607 (2018).
[3]D. P. Brunco, B. D. Jaeger, G. Eneman, J. Mitard, G. Hellings, A. Satta, V. Terzieva, L. Souriau, F. E. Leys, G. Pourtois, M. Houssa, G. Winderickx, E. Vrancken, S. Sioncke, K. Opsomer, G. Nicholas, M. Caymax, A. Stesmans, J. Van Steenbergen, P. W. Mertens, M. Meuris, and M. M. Heyns, "Germanium MOSFET devices: Advances in materials understanding, process development, and electrical performance," J. Electrochem. Soc. **155**, H552 (2008).
[4]V. Voronkov and R. Falster, "Vacancy-type microdefect formation in czochralski silicon," J. Cryst. Growth **194**, 76–88 (1998).
[5]T. Südkamp and H. Bracht, "Self-diffusion in crystalline silicon: A single diffusion activation enthalpy down to 755 °C," Phys. Rev. B **94**, 125208 (2016).
[6]N. Fukata, A. Kasuya, and M. Suezawa, "Vacancy formation energy of silicon determined by a new quenching method," Jpn. J. Appl. Phys. **40**, L854 (2001).
[7]H. M. Pinto, J. Coutinho, V. J. B. Torres, S. Öberg, and P. R. Briddon, "Formation energy and migration barrier of a Ge vacancy from ab initio studies," Mater. Sci. Semicond. Process. **9**, 498–502 (2006).
[8]A. J. R. da Silva, A. Janotti, A. Fazzio, R. J. Baierle, and R. Mota, "Self-interstitial defect in germanium," Phys. Rev. B **62**, 9903–9906 (2000).
[9]M. Werner, H. Mehrer, and H. D. Hochheimer, "Effect of hydrostatic pressure, temperature, and doping on self-diffusion in germanium," Phys. Rev. B **32**, 3930–3937 (1985).
[10]I. Riihimäki, A. Virtanen, S. Rinta-Anttila, P. Pusa, and J. Räisänen, and The ISOLDE Collaboration, "Vacancy-impurity complexes and diffusion of Ga and Sn in intrinsic and *p*-doped germanium," Appl. Phys. Lett. **91**, 091922 (2007).
[11]A. Chroneos, H. Bracht, R. W. Grimes, and B. P. Uberuaga, "Vacancy-mediated dopant diffusion activation enthalpies for germanium," Appl. Phys. Lett. **92**, 172103 (2008).
[12]S. Schneider, H. Bracht, J. N. Klug, J. L. Hansen, A. N. Larsen, D. Bougeard, and E. E. Haller, "Radiation-enhanced self- and boron diffusion in germanium," Phys. Rev. B **87**, 115202 (2013).
[13]S. Yamaoka, K. Kobayashi, K. Sueoka, and J. Vanhellemont, "Density functional theory study of dopant effect on formation energy of intrinsic point defects in germanium crystals," J. Cryst. Growth **474**, 104–109 (2017).
[14]H. Bracht, S. Schneider, and R. Kube, "Diffusion and doping issues in germanium," Microelectron. Eng. **88**, 452–457 (2011).
[15]H. Bracht, S. Schneider, J. N. Klug, C. Y. Liao, J. L. Hansen, E. E. Haller, A. N. Larsen, D. Bougeard, M. Posselt, and C. Wündisch, "Interstitial-mediated diffusion in germanium under proton irradiation," Phys. Rev. Lett. **103**, 255501 (2009).
[16]E. Simoen and J. Vanhellemont, "On the diffusion and activation of ion-implanted n-type dopants in germanium," J. Appl. Phys. **106**, 103516 (2009).
[17]A. Chroneos, R. W. Grimes, B. P. Uberuaga, and H. Bracht, "Diffusion and defect reactions between donors, C, and vacancies in Ge. II. Atomistic calculations of related complexes," Phys. Rev. B **77**, 235208 (2008).
[18]H. Bracht, H. H. Silvestri, I. D. Sharp, and E. E. Haller, "Self- and foreign-atom diffusion in semiconductor isotope heterostructures. II. Experimental results for silicon," Phys. Rev. B **75**, 035211 (2007).
[19]A. Fazzio, A. Janotti, A. J. R. da Silva, and R. Mota, "Microscopic picture of the single vacancy in germanium," Phys. Rev. B **61**, R2401–R2404 (2000).
[20]T. Südkamp, H. Bracht, G. Impellizzeri, J. Lundsgaard Hansen, A. Nylandsted Larsen, and E. E. Haller, "Doping dependence of self-diffusion in germanium and the charge states of vacancies," Appl. Phys. Lett. **102**, 242103 (2013).

[21]N. Kuganathan, H. Bracht, K. Davazoglou, F. Kipke, and A. Chroneos, "Impact of oxygen on gallium doped germanium," AIP Adv. **11**, 065122 (2021).
[22]A. Chroneos and H. Bracht, "Diffusion of *n*-type dopants in germanium," Appl. Phys. Rev. **1**, 011301 (2014).
[23]A. Chroneos, B. P. Uberuaga, and R. W. Grimes, "Carbon, dopant, and vacancy interactions in germanium," J. Appl. Phys. **102**, 083707 (2007).
[24]J. Slotte, S. Kilpeläinen, F. Tuomisto, J. Räisänen, and A. N. Larsen, "Direct observations of the vacancy and its annealing in germanium," Phys. Rev. B **83**, 235212 (2011).
[25]K. Kuitunen, F. Tuomisto, J. Slotte, and I. Capan, "Divacancy clustering in neutron-irradiated and annealed *n*-type germanium," Phys. Rev. B **78**, 033202 (2008).
[26]J. Slotte, K. Kuitunen, S. Kilpeläinen, F. Tuomisto, and I. Capan, "Divacancies at room temperature in germanium," Thin Solid Films **518**, 2314–2316 (2010).
[27]M. Christian Petersen, A. Nylandsted Larsen, and A. Mesli, "Divacancy defects in germanium studied using deep-level transient spectroscopy," Phys. Rev. B **82**, 075203 (2010).
[28]A. N. Subramanian, M. P. Kabukcuoglu, C. Richter, U. Juda, R. Kernke, F. Bärwolf, E. Hamann, M. Zuber, N. V. Abrosimov, and R. R. Sumathi, "Growth of boron-doped germanium single crystals by the Czochralski method," Cryst. Growth Des. **25**, 1075–1081 (2025).
[29]A. Subramanian, N. Abrosimov, A. Gybin, C. Guguschev, U. Juda, A. Fiedler, F. Bärwolf, I. Costina, A. Kwasniewski, A. Dittmar, and R. R. Sumathi, "Investigation of doping processes to achieve highly doped Czochralski germanium ingots," J. Electron. Mater. **52**, 5178–5188 (2023).
[30]F. Tuomisto and I. Makkonen, "Defect identification in semiconductors with positron annihilation: Experiment and theory," Rev. Mod. Phys. **85**, 1583–1631 (2013).
[31]J. F. Ziegler, M. Ziegler, and J. Biersack, "SRIM—The stopping and range of ions in matter (2010)," Nucl. Instrum. Methods Phys. Res., Sect. B **268**, 1818–1823 (2010).
[32]R. Krause-Rehberg and H. Leipner, *Positron Annihilation in Semiconductors: Defect Studies* (Springen, Berlin, Heidelberg, 1999).
[33]Vl. Kolkovsky, M. Christian Petersen, A. Nylandsted Larsen, and A. Mesli, "No trace of divacancies at room temperature in germanium," Mater. Sci. Semicond. Process. **11**, 336–339 (2008).
[34]J. Kujala, N. Segercrantz, F. Tuomisto, and J. Slotte, "Native point defects in GaSb," J. Appl. Phys. **116**, 143508 (2014).
[35]C. Rauch, F. Tuomisto, P. D. C. King, T. D. Veal, H. Lu, and W. J. Schaff, "Self-compensation in highly n-type InN," Appl. Phys. Lett. **101**, 011903 (2012).